Structure–function studies of tryptophan mutants of equinatoxin II, a sea anemone pore-forming protein

Petra MALOVRH*, Ariana BARLIČ*, Zdravko PODLESEK*, Peter MAČEK*, Gianfranco MENESTRINA† and Gregor ANDERLUH*[1]

*Department of Biology, Biotechnical Faculty, University of Ljubljana, Večna pot 111, 1000 Ljubljana, Slovenia, and †CNR-ITC Centro di Fisica degli Stati Aggregati, Via Sommarive 18, 38050 Povo (Trento), Italy

Equinatoxin II (EqtII) is a eukaryotic cytolytic toxin that avidly creates pores in natural and model lipid membranes. It contains five tryptophan residues in three different regions of the molecule. In order to study its interaction with the lipid membranes, three tryptophan mutants, EqtII Trp^{45}, EqtII $Trp^{116/117}$ and EqtII Trp^{149}, were prepared in an *Escherichia coli* expression system [here, the tryptophan mutants are classified according to the position of the remaining tryptophan residue(s) in each mutated protein]. They all possess a single intrinsic fluorescent centre. All mutants were less haemolytically active than the wild-type, although the mechanism of erythrocyte damage was the same. EqtII $Trp^{116/117}$ resembles the wild-type in terms of its secondary structure content, as determined from Fourier-transform infrared (FTIR) spectra and its fluorescent properties. Tryptophans at these two positions are buried within the hydrophobic interior of the protein, and are transferred to the lipid phase during the interaction with the lipid membrane. The secondary structure of the other two mutants, EqtII Trp^{45} and EqtII Trp^{149}, was altered to a certain extent. EqtII Trp^{149} was the most dissimilar from the wild-type, displaying a higher content of random-coil structure. It also retained the lowest number of nitrogen-bound protons after exchange with ^2H_2O, which might indicate a reduced compactness of the molecule. Tryptophans in EqtII Trp^{45} and EqtII Trp^{149} were more exposed to water, and also remained as such in the membrane-bound form.

Key words: actinoporin, *Actinia equina*, lipid membranes, fluorescence, FTIR spectroscopy.

INTRODUCTION

Pore-forming toxins (PFTs) are probably the most ubiquitous protein toxins in Nature. The most well-known and studied examples are those of bacterial origin [1]. Equinatoxin II (EqtII), however, is an example of a eukaryotic PFT, which are, in general, less well studied. It is a major constituent of the venom of the sea anemone *Actinia equina* L., and belongs to a group of sea anemone lysins, collectively called actinoporins in view of their common characteristics [2,3]. These are $\approx$ 20 kDa proteins with high pIs, which are readily inhibited by sphingomyelin (SM), which acts as a membrane acceptor [4]. A comparison of the primary structures of actinoporins shows a high degree of internal identity, but no similarity to other proteins [5]. They act on natural and model lipid membranes by forming cation-selective channels with a hydrodynamic diameter of approx. 2 nm [6,7]. The mechanism of pore formation involves at least two steps: binding of the water-soluble monomer to the membrane, and oligomerization of monomers leading to the formation of a functional pore. A recent model of the membrane bound monomer envisages that the N-terminal helix 11–33, the hydrophobic region 105–120 (see Figure 1), and residues Arg^{144}, Ser^{160} and those nearby, interact with the lipid membrane [8]. Of particular interest is the amphiphilic α-helix at the N-terminal. It was proposed that this helix is involved in the interaction with the lipid membrane [9], although not a requisite for binding [10]. A conformational change(s) could expose hydrophobic regions of this molecule normally not accessible to the solvent [8,9,11], but the nature of these changes and the regions of the toxin molecule that participate in them are, at present, unknown.

Membrane proteins generally have aromatic residues located in the water–lipid interface [12–15]; the same has been observed for pore-forming peptides, e.g. gramicidin [16] and the heptameric channel formed by staphylococcal α-toxin [17], where tryptophan and tyrosine residues are mainly located in the rim domain partially inserted into the lipid membrane [18]. EqtII has five

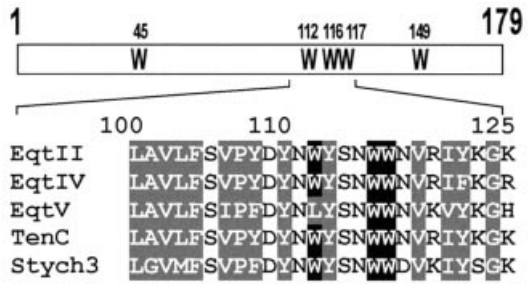

Figure 1 Location of tryptophan residues in EqtII

The numbers above the diagrammatic box indicate the five tryptophan residues. The sequence of the region containing a conserved tryptophan-rich cluster (amino acids 112–117) is shown below for all known actinoporins. The numbering is on the basis of the EqtII sequence. The aligned sequences are from EqtII (GeneBank accession number U41661), EqtIV (AF057028) and EqtV (U51900), all from *A. equina*; tenebrosin C (TenC) (SwissProt accession number P17723) from *A. tenebrosa*; and sticholysin III (Stych3) (P07845) from *S. helianthus*. Hydrophobic residues (L, A, V, I, P, G, F and Y) are shaded grey; tryptophan residues are shown in black.

Abbreviations used: ATR, attenuated total reflection; BRBC, bovine red blood cells; DPPC, 1,2-dipalmitoyl-*sn*-glycero-3-phosphocholine; EqtII, equinatoxin II; FTIR, Fourier-transform infrared; GdmCl, guanidinium chloride; NBS, *N*-bromosuccinimide; PFO, perfringolysin O; PFT, pore-forming toxins; β-py-C_{10}-HPC, 1-hexadecanoyl-2-(1-pyrenedecanoyl)-*sn*-glycero-3-phosphocholine; SM, sphingomyelin; SUV, small unilamellar vesicles.

[1] To whom correspondence should be addressed (e-mail: gregor.anderluh@uni-lj.si).

tryptophan residues located in three different parts of the molecule (Figure 1). Trp^{45} and Trp^{149} are located in a rather hydrophilic environment, whereas Trp^{112}, Trp^{116} and Trp^{117} belong to a hydrophobic region located in the middle of the protein (as predicted by hydropathy plot analysis [9]). Tryptophan emission fluorescence of the wild-type EqtII is indicative of a globular protein where tryptophan residues are buried in the interior of the protein [4]. However, the five tryptophan residues exhibit a different nature. A small number of them (probably two) are moderately well exposed, and accessible for chemical modification with *N*-bromosuccinimide (NBS) or 2,2′-azobis(2-amidinopropane) [19,20]. After modification, the toxin loses activity, but it seems that these solvent-exposed tryptophan residues are not involved in the binding to the membrane. The exposed tryptophan residues are also involved in 8-anilino-1-naphthalenesulphonate binding [21]. On the other hand, about three tryptophan residues are transferred into the bilayer after association with lipids, becoming inaccessible for quenching with acrylamide [4,20].

In order to determine in more detail both the structural importance and position of tryptophan residues in the membrane-bound form of EqtII, we have prepared three mutants each with single, intact fluorescent centres. The non-mutated tryptophan residues were used as intrinsic reporters in fluorescence studies of EqtII both in solution and in the lipid membrane. The results indicate that the 'tryptophan cluster' (residues 112–117) has a role both in maintaining the structure of the protein and in the initial interaction with the lipid membrane. In contrast, Trp^{45} and Trp^{149}, and residues proximal to these, are always solvent-exposed, but may have a role in later steps of pore formation.

MATERIALS AND METHODS

Materials

Restriction and DNA-modifying enzymes were purchased from Boehringer Mannheim (Mannheim, Germany) or New England Biolabs (Schwalbach, Germany). Oligonucleotides were purchased from The Great American Gene Company (Ramona, CA, U.S.A.). Guanidinium chloride (GdmCl) was a product from Serva (Heidelberg, Germany) and acrylamide was purchased from Bio-Rad (Hercules, CA, U.S.A.). All other chemicals of analytical grade were obtained from Sigma (St. Louis, MO, U.S.A.), Serva or Kemika (Zagreb, Croatia). SM and 1,2-dipalmitoyl-*sn*-glycero-3-phosphocholine (DPPC) were purchased from Avanti Polar Lipids (Alabaster, AL, U.S.A.). 1-Hexadecanoyl-2-(1-pyrenedecanoyl)-*sn*-glycero-3-phosphocholine (β-py-C_{10}-HPC) was obtained from Molecular Probes (Eugene, OR, U.S.A.).

Cloning of mutants

Three tryptophan mutants of EqtII were prepared by site-directed mutagenesis. The wild-type contains five tryptophan residues at positions 45, 112, 116, 117 and 149 (Figure 1). Here, and subsequently, the tryptophan mutants are referred to by the position of the remaining tryptophan residue(s) in each mutated protein, i.e. EqtII Trp^{45}, EqtII $Trp^{116/117}$ and EqtII Trp^{149}. The coding regions for tryptophan mutants were amplified by PCR from plasmid pAG2.1, coding for the wild-type EqtII, as described previously [22]. The 5′ and 3′ primers used were, in all cases, T7 (5′-TAATACGACTCACTATAG-3′) and T7-40 (5′-GTTTACTCATATATACTTTAG-3′) respectively. The production of mutants involved repetitive PCR reactions. In one step, in addition to T7 and T7-40 oligonucleotides, one of the following mutagenic primers [23] was also used in the reaction mix: $Trp^{112} \rightarrow$ Phe (5′-CCTATGACTATAACTTCTACAGCA-ACTGG-3′), $Trp^{116/117} \rightarrow$ Phe (5′-TACAGCAACTTCTTCAA-TGTCAGG-3′) and $Trp^{149} \rightarrow$ Phe (5′-GGGACAATGGCT-TCCACACCAGGAATC-3′) for the mutant EqtII Trp^{45}; $Trp^{45} \rightarrow$ Phe (5′-CGGGCAAGACGTTCACCGCATTGAAC-3′), $Trp^{112} \rightarrow$ Phe and $Trp^{149} \rightarrow$ Phe for mutant EqtII $Trp^{116/117}$; and $Trp^{45} \rightarrow$ Phe, $Trp^{112} \rightarrow$ Phe and $Trp^{116/117} \rightarrow$ Phe for the mutant EqtII Trp^{149}. PCR products were digested with *Nde*I and *Eco*RI, and cloned into a pT7-7 expression vector. The entire coding region for each mutant was checked for errors introduced by the *Taq* polymerase using a T7 sequencing kit (Pharmacia; Piscataway, NJ, U.S.A.) and deoxyadenosine 5′-[α-^{35}S]triphosphate (Amersham, Little Chalfont, Bucks., U.K.).

Expression and isolation of mutants

The constructed vectors were used to transform the *Escherichia coli* BL21(DE3) strain and the expression of EqtII mutants was induced as described previously [22]. After expression, the cells were spun down and resuspended in phosphate buffer, pH 7.2. After 30 min of vigorous shaking at 4 °C, the suspension was sonicated on ice for 3 min at 70 W using an MSE 150 W ultrasonic disintegrator. The procedure was repeated up to six times; in later steps, 0.1 % (v/v) Triton X-100 was added to the suspension. The wild-type and mutant proteins were isolated as described previously [22,24].

Determination of protein concentration

Protein concentration was determined spectrophotometrically by measuring the absorbance at 280 nm. Absorption coefficients were calculated, taking into account the number of tryptophan and tyrosine residues in the proteins as described by the method of Perkins [25]. Calculated specific absorption coefficients, $A^{1\%}_{1cm}$, used were 2.21 for the wild-type, 1.35 for EqtII $Trp^{116/117}$ and 1.06 for both EqtII Trp^{45} and EqtII Trp^{149}.

Haemolytic activity

Haemolytic activity was measured in terms of attenuance on bovine red blood cells (BRBC) at 25 °C using a microplate reader (MRX; Dynex Technologies, Denkendorf, Germany). Toxins at desired concentrations were added in the first well to erythrocyte buffer (0.13 M NaCl/0.02 M Tris/HCl, pH 7.4), and then serially diluted 2-fold. BRBC (100 μl; $D_{630} = 0.5$) in erythrocyte buffer were added to the toxins, and haemolysis was monitored by measuring attenuance at 630 nm for 20 min at room temperature. The final volume in all wells was 200 μl. The percentage of haemolysis was determined at the end of the assay using the following equation:

$$\text{Haemolysis } (\%) = (D_{max} - D_{obs})/(D_{max} - D_{min}) \times 100 \quad (1)$$

in which D_{obs} was the measured attenuance in the well after 20 min and D_{max} and D_{min} were the maximal and the minimal attenuances respectively.

Preparation of lipid vesicles

Liposomes were formed either of SM and DPPC (1:1, mol/mol) or of SM, DPPC and β-py-C_{10}-HPC (49:49:2, by mol). Chloroform was removed from the lipid mixture with a rotary evaporator. Vesicle buffer (140 mM NaCl, 20 mM Tris/HCl, 1 mM EDTA, pH 8.5) was added to the lipid film to give a final lipid

concentration of 2 mg/ml, and the suspension was vortex-mixed vigorously. Small unilamellar vesicles (SUV) were prepared by sonication (MSE 150 W ultrasonic disintegrator), applying 20-s pulses for 30 min (output scale 6) at room temperature. The liposomes were incubated at 45 °C for approx. 1 h to complete the annealing process. The vesicle suspension was then centrifuged at 28000 ***g*** for 20 min in a 3K30 centrifuge (Sigma, Deisenhofen, Germany) to remove titanium particles released from the probe, and the supernatant was stored at 4 °C for up to 3 days before use.

Binding to red blood cells and SUV

Toxins at a final concentration of 76 nM (or 760 nM in the case of mutant EqtII Trp^{149}) were incubated in erythrocyte buffer with 50 μl of BRBC ($D_{630} = 0.5$) in a total volume of 100 μl for 10 min. Thereafter, 100 μl of BRBC ($D_{630} = 0.5$) was added and haemolysis was measured as described above. The amount of unbound toxin was determined by estimating its residual haemolytic activity. The binding to SUV (DPPC/SM, 1:1 by mol) was assayed similarly. Toxins were preincubated with SUV corresponding to a lipid:toxin ratio of 10, 100 or 600 for 2 min, BRBC were then added, and the residual haemolytic activity was measured.

Fluorescence spectroscopy

All fluorescence measurements were performed using a Jasco FP-750 spectrofluorimeter (Jasco Corporation, Tokyo, Japan). The sample compartment was equipped with a magnetic stirrer and a Peltier thermostatted single-cell holder. Unless stated otherwise, fluorescence measurements were performed at 25 °C in 50 mM Tris/HCl, pH 8.0, at a toxin concentration of 250 nM. No further correction for wavelength dependence of the photomultiplier tube was made. Steady-state tryptophan emission spectra were measured by excitation at 295 nm to minimize tyrosine emission [26]. Fluorescence emission was scanned from 310–400 nm at 60 nm/min, with excitation and emission slits set at 5 nm. The spectrum of buffer alone was measured under the same conditions and subtracted from the sample emission. For measurements of the kinetics of toxin binding to SUV, the excitation wavelength was set at 295 nm, whereas emission wavelengths were set at 334 nm, 345 nm, 336 nm and 359 nm for the wild-type, EqtII Trp^{45}, EqtII $Trp^{116/117}$ and EqtII Trp^{149} proteins respectively. The apertures of the slits were 5 nm on both beams. To 250 nM toxin in 140 mM NaCl, 20 mM Tris/HCl, 1 mM EDTA, pH 8.5, appropriate amounts of SUV either with or without quencher were added. The intensities were corrected for the dilution factor, and the background was subtracted using the appropriate blanks with SUV only. The rate constant for binding of the wild-type and mutant EqtII $Trp^{116/117}$ to SUV was derived by fitting experimental fluorescence data to the single-exponential function:

$$F = F_{max}(1 - e^{-kt}) \quad (2)$$

where F is the fluorescence at time t, F_{max} the asymptotic value at infinite t, and k the rate constant. The quenching efficiency, E, for quenching of tryptophan fluorescence by pyrene in SM/DPPC/β-py-C_{10}-HPC SUV was calculated as follows:

$$E = 1 - (F_{SM/DPPC/\beta\text{-py-C10-HPC}}/F_{SM/DPPC}) \quad (3)$$

where $F_{SM/DPPC/\beta\text{-py-C10-HPC}}$ is the fluorescence intensity in the presence of SM/DPPC/β-py-C_{10}-HPC SUV, and $F_{SM/DPPC}$ is the fluorescence intensity in the presence of SM/DPPC SUV.

Chemical modifications with NBS

Toxins at 1 μM concentration in 0.1 M sodium acetate buffer, pH 4.8, were incubated in a cuvette at 25 °C, and stirred continuously. Small aliquots of 1mM NBS in the same buffer were added and the fluorescence was measured as described above after 2 min of stirring. The fluorescence due to the buffer was subtracted from the observed spectra, and these were corrected further for the dilution. For effects of NBS on haemolytic activity, toxins at 200 nM were incubated in 0.1 M sodium acetate buffer, pH 4.8, with different concentrations of NBS in a total volume of 100 μl. The residual haemolytic activity was measured as described above after 10 min incubation at room temperature.

Quenching with acrylamide

Acrylamide was added from a 5 M stock solution to 250 nM toxin in 50 mM Tris/HCl, pH 8.0, at 25 °C. After each addition the solution was stirred for 1 min, and then tryptophan fluorescence spectra were measured as described above. They were corrected both for the emission of buffer alone and for the dilution introduced by acrylamide. The inner-filter effect was negligible at the acrylamide concentrations used. The quenching data were analysed using the Stern–Volmer equation [27]:

$$F_0/F = 1 + K_{sv}[Q] \quad (4)$$

where F_0 is the fluorescence of the protein in the absence of acrylamide, F is the observed fluorescence, [Q] is the concentration of acrylamide, and K_{sv} is the collisional quenching constant. For the wild-type protein, a modified Stern–Volmer equation for multiple emitting centres was used [4,26,27]:

$$F_0/\Delta F = 1/(f_a K_{sv}[Q]) + 1/f_a \quad (5)$$

where f_a is the maximal fraction of accessible fluorescence and ΔF is the difference between the initial fluorescence and that after quenching.

Fourier-transform infrared (FTIR) spectroscopy

FTIR spectra were collected on a Bio-Rad FTS 185 spectrometer equipped with a deuterium triglycine sulphate (DTGS) detector featuring a CsI window and KBr beam-splitter. The instrument was purged with CO_2-free dry air. The attenuated total reflection (ATR) configuration was used [28] with a 10-reflection Ge crystal, as described previously [11,29]. Absorption spectra were obtained in the region between 4000 and 600 cm^{-1}, at a resolution of one datum point every 0.25 cm^{-1}, using a clean crystal as a background. Toxins (40 μg of 25 μM concentration dissolved in water) were deposited on one side of a crystal, and gently dried under nitrogen in a thin layer. Thirty interferograms were collected, Fourier-transformed, and then averaged. After collecting spectra in a water-saturated environment, the crystal was flushed with ^2H_2O-saturated nitrogen for 20–30 min to allow deuteration of the fast-exchangeable amide hydrogen ions, and deuterated spectra were subsequently collected. ATR–FTIR spectra were processed using the Bio-Rad Win-Ir software package. First, the residual water vapour features were removed; then, the amide I′ band between 1700 and 1600 cm^{-1} was deconvoluted, and the number, position, amplitude and width of its Lorentzian components were determined. These were used as starting parameters for a final recursive refinement on the basis of a least-squares fit of the original spectrum as described by the Levenberg–Marquardt method [29]. The relative contents of secondary structural elements were finally estimated by dividing

the areas of the individual components assigned to a particular secondary structure in the standard manner [30] by the area of the whole amide I′ band. The two small components around 1614 and 1600 cm^{-1}, arising from the contribution of the side chains, were excluded from the sum [11,29,31]. The area of the amide A-band, arising from the νN–H stretch, was calculated after best fit with a single Lorentzian component centred at 3291 ± 1 cm^{-1} [32].

RESULTS

Characterization of tryptophan mutants

Three tryptophan mutants of EqtII were prepared by site-directed mutagenesis, overexpressed, and purified as described previously for the wild-type [22]. The purified toxins were more than 95% homogeneous, as estimated by SDS/PAGE, and showed the same migration as that of native EqtII (results not shown). The yields of EqtII Trp^{45} and EqtII Trp^{149} were slightly lower, while that of EqtII $Trp^{116/117}$ corresponded to that of the wild-type [22] (Table 1). As found for the wild-type protein, all mutants were soluble up to the highest concentrations used in the present study.

Figure 2(A) shows the percentage of haemolysis (calculated using eqn. 1) as a function of the toxin concentration. The concentration of the protein needed to produce 50% of haemolysis (c_{50}) was determined from such curves and its reciprocal, c_{50}^{-1}, was used to express toxin activity, as reported in Table 1. All mutants were less haemolytically active than the wild-type. The activity of EqtII $Trp^{116/117}$ was about 31% of that of the wild-type, while EqtII Trp^{45} and EqtII Trp^{149} were even less active, expressing only 7% and 2% of the wild-type activity respectively. Although the loss of haemolytic activity was considerable for both EqtII Trp^{45} and EqtII Trp^{149}, the kinetics of haemolysis remained the same. The time course for BRBC haemolysis observed with 8 nM of the wild-type protein was the same as that obtained with the mutants, albeit with the mutant proteins being present at higher concentrations: 78, 19.5 and 390 nM for EqtII Trp^{45}, EqtII $Trp^{116/117}$ and EqtII Trp^{149} respectively (Figure 2B). Furthermore, very similar Hill coefficients (Table 1) suggest that the mechanism by which EqtII lyses erythrocytes, i.e. a colloidal osmotic shock ensuing from pore formation, is also conserved in the mutant proteins.

In order to see whether the reduced haemolytic activity is a consequence of a reduced binding ability, the binding of proteins to BRBC and SUV was measured. All toxins were able to bind to erythrocytes and SUV (Table 1), but EqtII Trp^{45} and EqtII Trp^{149} showed reduced binding to BRBC, whereas the binding of EqtII $Trp^{116/117}$ was unchanged (Table 1). Similar results were obtained with SUV when the lipid:toxin ratio was 10:1, whereas at the ratios of 100:1 and 600:1 (Table 1) the differences

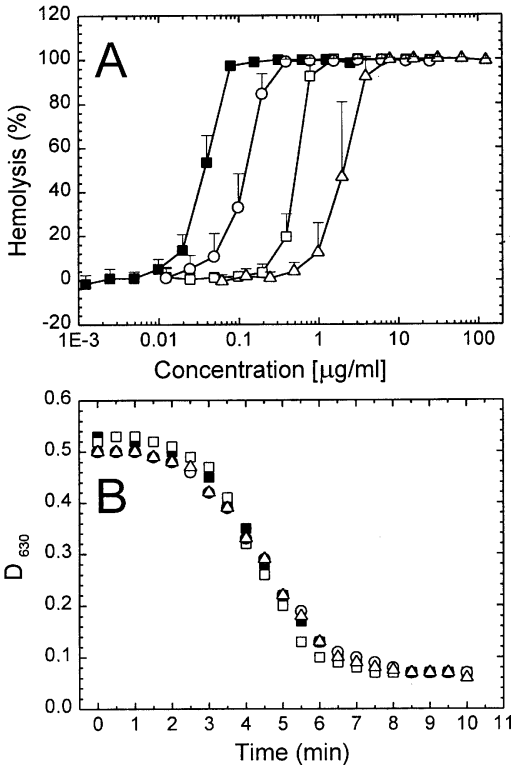

Figure 2 Haemolysis of BRBC caused by the wild-type and tryptophan mutants

(**A**) Titration of haemolytic activity. Haemolysis was measured turbidimetrically at room temperature using an automated microplate reader. The final percentage of haemolysis was calculated as described in the Materials and methods section. Data points shown are means + S.D. for six independent experiments. (**B**) Time course of haemolysis. The protein concentrations were 8, 78, 19.5 and 390 nM for the wild-type (■), EqtII Trp^{45} (□), EqtII $Trp^{116/117}$ (○) and EqtII Trp^{149} (△) proteins respectively.

Table 1 Characteristics of EqtII and tryptophan mutants

Hill coefficients (h) were determined from the dependence of the rate of haemolysis on the toxin concentration. F and F_0 are intensities at λ_{max} of initial fluorescence and fluorescence after addition of NBS respectively. Values shown are means ± S.D. a.u., arbitrary units.

						Tryptophan fluorescence			
						Native		NBS modified*	
Protein	Yield (mg/l)	$1/c_{50}$ (pM^{-1}) ($n = 6$)	h ($n = 6$)	Binding to BRBC (%) ($n = 2$)	Binding to SUV lipid/toxin 100 (%) ($n = 2$)	λ_{max} (nm) ($n = 4$)	$F_{\lambda max}$ (a.u.) ($n = 4$)	λ_{max} (nm) ($n = 2$)	F/F_0 (%) ($n = 2$)
Wild-type	1.00 [22]	547.4 ± 88.2	1.18 ± 0.02	98.7 ± 0.1	78.2 ± 10.9	339 ± 1	73.1 ± 5.2	332 ± 1	27 ± 2
EqtII Trp^{45}	0.7	38.1 ± 3.3	1.29 ± 0.01	53.5 ± 7.5	67.3 ± 2.1	347 ± 2	13.4 ± 1.4	347 ± 1	1.7 ± 1.0
EqtII $Trp^{116/117}$	1.1	169.8 ± 37.4	1.23 ± 0.02	99.3 ± 0.1	88 ± 1.4	338 ± 1	23.1 ± 3.6	338 ± 1	16 ± 3
EqtII Trp^{149}	0.8	10.5 ± 4.1	1.22 ± 0.08	73.3 ± 0.3	86.8 ± 2.4	355 ± 1	9.7 ± 0.5	355 ± 1	2.5 ± 0.5

* Steady-state values at an NBS/protein ratio of 14.

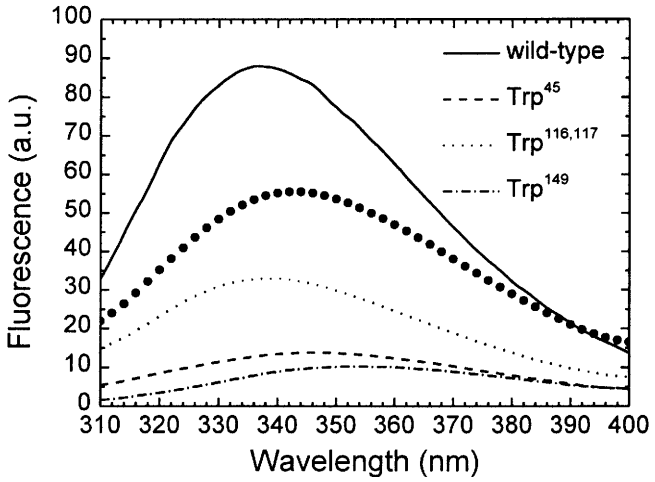

Figure 3 Fluorescence emission spectra of the wild-type and tryptophan mutants

Toxins at 250 nM concentration in 50 mM Tris/HCl, pH 8, at 25 °C were scanned. The excitation wavelength was set at 295 nm; excitation and emission slits were set at 5 nm. The summed spectra of EqtII Trp^{45}, EqtII $Trp^{116/117}$ and EqtII Trp^{149} are represented by the trace with large dots (●●●●●●).

gradually disappeared. At a lipid:toxin ratio of 600:1, $> 92\%$ of all proteins were bound.

Intrinsic fluorescence of tryptophan mutants

Tryptophan emission spectra of the wild-type and mutant proteins are shown in Figure 3, and positions of the maxima are listed in Table 1. The fluorescence spectrum of the wild-type has features characteristic of tryptophan residues that are excluded from the solvent, with a λ_{max} of 339 nm (Table 1; also see [4]). The same spectral shape was observed with mutant EqtII $Trp^{116/117}$; however, the fluorescence intensity for this mutant was only 30 % of that of the wild-type (Figure 3). The other two mutants displayed a clear red shift of 8 and 16 nm for EqtII Trp^{45} and EqtII Trp^{149} respectively, and a strong decrease in fluorescence intensity (Table 1). This clearly demonstrates that the indolyl side chain in these two mutants is exposed to the solvent. In the case of EqtII Trp^{149}, it was probably completely exposed, since no further spectral change could be observed when this mutant was denatured either thermally or with GdmCl. The sum of fluorescence intensities of the mutants, comprising four of the original five tryptophan residues, was around 59 % of that of the wild-type, with a λ_{max} at 343 nm (Figure 3). This suggests that the individual contributions of the tryptophan residues in the wild-type are not additive by a simple relationship, and/or that the mutants may have different conformations. Upon denaturation, either with 6 M GdmCl or with temperature, the spectra of all mutants, as found for the wild-type, were red-shifted to 355 nm, indicating total exposure of tryptophan residues to water under these conditions (results not shown).

FTIR determination of the secondary structure of tryptophan mutants

The secondary structure of EqtII and mutants was assayed by IR spectroscopy [32,33], a method already employed with other actinoporins of the same family [11]. The amide I′ vibrational band of EqtII, and its deconvolution, are shown in Figure 4. The deconvolved spectrum is dominated by a peak at 1636 cm^{-1},

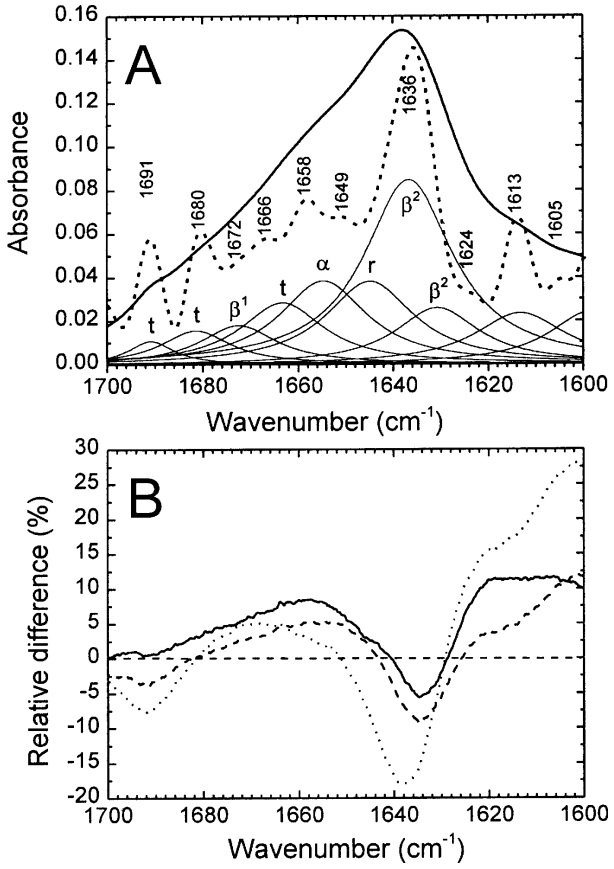

Figure 4 Amide I′ IR–ATR spectra of deuterated films of the wild-type and tryptophan mutants

(**A**) The spectrum (thick continuous line) and its deconvolution, obtained using a resolution enhancement factor $k = 2$ (dotted line), are shown for EqtII. The positions of ten components are apparent on the deconvoluted spectrum. These components were used as starting values for curve-fitting the original spectrum with ten Lorentzian bands, as explained in the Materials and methods section. The best-fitted components (thinner continuous lines) were assigned to secondary structures as described previously [30], and the assignments are indicated. The following criteria were used: bands in the regions 1691–1680 cm^{-1} and 1665–1661 cm^{-1}, β-turn (t); band at 1672 ± 1 cm^{-1}, antiparallel β-sheet (β^1 band); band at 1654 ± 1 cm^{-1}, α-helix (α); band at 1645 ± 1 cm^{-1}, random coil (r); bands in the region 1638–1625 cm^{-1}, parallel plus antiparallel β-sheet (β^2 bands). The minor bands around 1614 cm^{-1} and 1600 cm^{-1} were attributed to side chains [31]. The evaluated secondary structures of the wild-type and mutants are reported in Table 2. (**B**) Relative differential spectra obtained by subtracting the amide I′ band of the wild-type (weighted by a suitable factor) from that of the mutants. The weight was calculated by dividing the area of the amide I′ band of the mutant by that of the wild-type. The amplitudes of the difference spectra were reported as a percentage of the amplitude of the mutant amide I′ band. EqtII Trp^{45}, continuous line; EqtII $Trp^{116/117}$, dashed line; EqtII Trp^{149}, dotted line.

which indicates the predominance of an extended β structure [32,33]. Furthermore, all the other peaks present could be assigned to secondary structure elements, and the relative content of each of them was estimated by the relative area of the corresponding Lorentzian curve, fitted to the original spectrum (see Figure 4 and ref. [11]). The average compositions determined in this manner are shown in Table 2. In agreement with previous CD spectroscopy experiments [9,34], and with FTIR spectroscopic analysis of two similar actinoporins from *Stichodactyla helianthus* [11], EqtII possesses a large amount of β structure, comprising $\approx 50\%$ β-sheet and 18 % β-turn, with only $\approx 16\%$

Table 2 FTIR spectroscopic determination of the secondary structure of wild-type and tryptophan mutants

The secondary structure elements were calculated as shown in Figure 4. Relative errors of these determinations were typically ±5%. The standard deviations derived from several independent fits were always smaller than this margin. The number of remaining nitrogen-bound protons after flushing the sample with ^2H_2O-saturated nitrogen was estimated as the ratio between the area of the amide A band (3291 cm^{-1}) and that of the amide I′ band (1600–1700 cm^{-1}). $\beta_{tot} = \beta^1 + \beta^2$. T, β-turn.

Protein	β^1	β^2	T	α	r	β_{tot}	Amide A/amide I′
EqtII	6	44	18	16	16	50	0.42
EqtII Trp^{45}	7	42	18	18	15	49	0.38
EqtII $Trp^{116/117}$	7	42	19	17	15	49	0.42
EqtII Trp^{149}	8	34	20	18	20	42	0.07

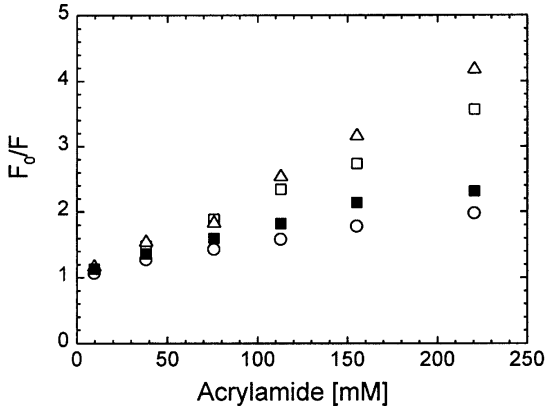

Figure 5 Stern–Volmer plots of acrylamide quenching

Acrylamide was added in aliquots to 250 nM toxins in 50 mM Tris/HCl, pH 8, at 25 °C. The excitation wavelength was set at 295 nm; slits were set at 5 nm. The mission maximum was 339 nm for the wild-type (■), 344 nm for EqtII Trp^{45} (□), 339 nm for EqtII $Trp^{116/117}$ (○), and 355 nm for EqtII Trp^{149} (△) respectively. The derived quenching constants (K_{SV}) are described in Table 3.

each of α-helix and random coil. Putative conformational changes resulting from the mutations were investigated by constructing differential spectra between the mutants and the wild-type. All mutants exhibited some changes, the most prominent of which was a decrease in absorbance around 1635–1637 cm^{-1}, indicative of a loss of secondary structure in the β^2 region (Figure 4B). However, the extent of such changes was different from mutant to mutant. In the case of EqtII Trp^{45} and EqtII $Trp^{116/117}$ the overall secondary structure, as evaluated by the curve-fit procedure, was only slightly affected (Table 2), since the β^1 structure increased slightly to compensate for the decrease in β^2 structure, while the α-helix and random coil components practically did not change. Instead, the spectrum of EqtII Trp^{149} was more severely affected, showing bigger changes at 1635–1637 cm^{-1}, but also a decrease at 1690 cm^{-1}, i.e. in one of the β-turn regions. In this case, the total amount of β structure had a relative decrease of 16%, and that of random coil showed a relative increase of 25%; in contrast, only minor changes were noted in α-helix and β-turn content (Table 2).

It was observed that extensively flushing the samples with ^2H_2O-saturated nitrogen could not exchange all of the protein-bound protons. In fact, all samples retained a clear N–H band at 3290 cm^{-1} (amide A). Interestingly, the relative amount of protons retained by each protein was variable, suggesting that this could provide a measure of the compactness of their structures (Table 2). In fact, the wild-type and EqtII $Trp^{116/117}$ proteins retained the highest amount of protons, with EqtII Trp^{45} retaining only slightly fewer, but EqtII Trp^{149} retained only very little. This would indicate that EqtII Trp^{149}, although retaining the major secondary structural features (as described above), adopted a protein fold markedly different from that of the wild-type, allowing a faster exchange of all protons for deuterons. The same applies for EqtII Trp^{45}, albeit to a less pronounced extent, while EqtII $Trp^{116/117}$ appeared to be folded normally.

Acrylamide quenching of tryptophan mutants

Stern–Volmer plots for acrylamide quenching of the wild-type and mutants are shown in Figure 5. At the highest concentration of quencher used (940 mM), the remaining fluorescence measurements were 16.1, 4.0, 14, and 2.7% of those found in the absence of quencher for the wild-type, EqtII Trp^{45}, EqtII $Trp^{116/117}$ and EqtII Trp^{149} proteins respectively, indicating that tryptophan residues of EqtII Trp^{45} and EqtII Trp^{149} are more exposed than those of EqtII $Trp^{116/117}$, and are thus readily quenched. The values of the Stern–Volmer constants derived from the plots in Figure 5 are given in Table 3. Tryptophan residues in different mutants are partially accessible to solvent. EqtII Trp^{45} and EqtII Trp^{149} exhibit the largest constants, indicating higher accessibility to acrylamide and exposure to solvent than the wild-type or EqtII $Trp^{116/117}$. The K_{sv} value for EqtII $Trp^{116/117}$, being the lowest determined for the proteins, indicates that the location of these tryptophan residues in the protein interior prevents them from interacting with acrylamide. The accessibility factor, f_a, of 0.57 for the wild-type confirms further that a fraction of

Table 3 Quenching of tryptophan fluorescence of the wild-type and mutants by soluble and membrane-bound quenchers

Stern–Volmer constants (K_{SV}) of acrylamide quenching were determined as described in the Materials and methods section. The fraction of the wild-type tryptophan residues accessible for quenching (shown in parentheses) was determined by using the modified Stern–Volmer equation. The average ± S.D. of two independent experiments is shown. Fluorescence intensity (F) was that emitted by 250 nM protein bound to SUV composed of either SM/DPPC (1:1) or SM/DPPC/β-py-C_{10}-HPC (49:49:2) at a lipid/toxin ratio of 600. Quenching efficiency (E) was calculated as described in the Materials and methods section.

	K_{SV} (M^{-1}) in solution	$F_{(SM/DPPC)}$ (a.u.)	$F_{(SM/DPPC/\beta\text{-py-C10-HPC})}$ (a.u.) (membrane bound)	E (%)
Wild-type	7.6 ± 1.7 (0.57 ± 0.01)	99.7 ± 1.2	56 ± 5.9	43.8
EqtII Trp^{45}	10.1 ± 2.1	13 ± 0.4	12.2 ± 0.1	6.0
EqtII $Trp^{116/117}$	6.3 ± 2.0	29.9 ± 1.3	20.8 ± 2.5	30.7
EqtII Trp^{149}	13.5 ± 0.6	9.4 ± 0.2	8.8 ± 0.02	7.1

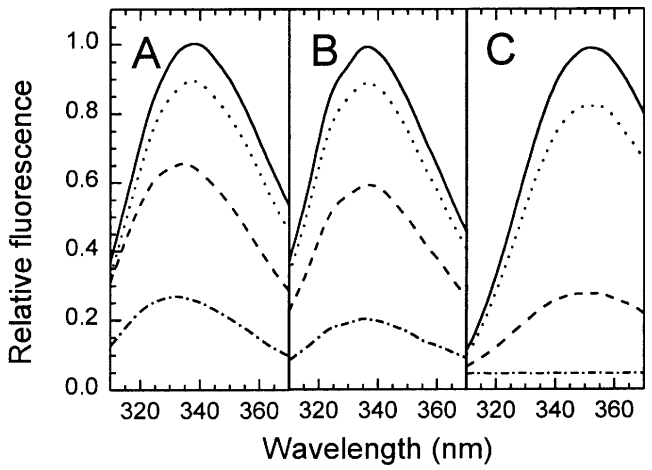

Figure 6 Chemical modifications of the wild-type and tryptophan mutants

Toxins at 1 μM concentration in 0.1 M sodium acetate, pH 4.8, were stirred at 25 °C. Aliquots of 1 mM NBS were added, stirred for 2 min and then fluorescence spectra were measured. The excitation wavelength was set at 295 nm; excitation and emission slits were set at 5 nm. Spectra are shown for the wild-type (**A**), Trp$^{116/117}$ (**B**) and EqtII Trp^{45} (**C**) proteins, with native toxins (continuous lines), or modified at an NBS/protein molar ratio of 2 (dotted lines), 5 (dashed lines) or 10 (dash–dotted lines). EqtII Trp^{149} behaved similarly to EqtII Trp^{45}.

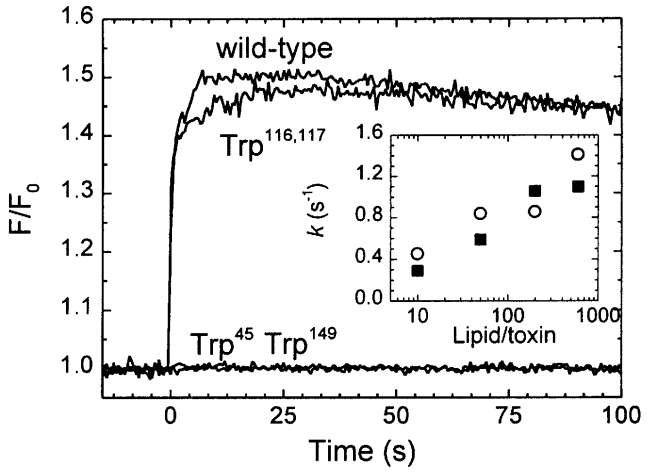

Figure 7 Kinetics of the increase of intrinsic tryptophan fluorescence of the wild-type and tryptophan mutants

Tryptophan fluorescence of 250 nM toxin (in 140 mM NaCl, 20 mM Tris/HCl, 1 mM EDTA, pH 8.5) was measured continuously after addition of SM/DPPC SUV at a lipid/toxin ratio of 600 at 25 °C. The excitation wavelength was set to 295 nm, and emission was scanned at 334 nm for the wild-type, 345 nm for EqtII Trp^{45}, 336 for EqtII Trp$^{116/117}$, and 355 nm for EqtII Trp^{149}. The inset shows the dependence of the rate constants of increase in tryptophan fluorescence for the wild-type (■) and EqtII Trp$^{116/117}$ (○) proteins on the lipid/toxin molar ratio. Rate constants were determined by fitting time courses of the increase of tryptophan fluorescence to eqn. (2).

tryptophan residues, $\approx 40\,\%$, is buried within the protein interior [4].

Chemical modifications of tryptophan mutants

Tryptophan residues in the wild-type and mutant proteins were oxidized using a tryptophan-specific reagent, NBS. The intrinsic fluorescence of all proteins was sensitive to NBS modification, showing a dose-dependent decrease (Figure 6). In the case of the wild-type, the maximal decrease was of $\approx 70\,\%$ in fluorescence, and was accompanied by a blue shift of the emission maximum (Figure 6 and Table 1). In contrast, with EqtII Trp^{45} and EqtII Trp^{149} the fluorescence almost completely disappeared, and no shift was observed in any of the intermediates. In the case of EqtII Trp$^{116/117}$, the fluorescence decreased by a maximum of $80\,\%$, without any shift. This is consistent with the view that tryptophans at positions 45 and 149 are both exposed, whereas those at positions 116 and 117 are less accessible. In the case of the wild-type protein, a blue shift results from the fact that tryptophans more exposed, which are red-shifted, are more readily and exhaustively modified. Consistent with previous results [19,20], tryptophan oxidation also led to a decrease in haemolytic activity. The concentrations of NBS at which toxins retained $50\,\%$ of activity, normalized per mol of tryptophan residues in each toxin, were 5.8, 27.6, 16.3 and 9 μM for the wild-type, EqtII Trp^{45}, EqtII Trp$^{116/117}$ and EqtII Trp^{149} proteins respectively.

Interaction of tryptophan mutants with SUV

Upon addition to SM/DPPC SUV at a lipid:toxin molar ratio of 600:1, an increase of the emitted tryptophan fluorescence was observed with both the wild-type and EqtII Trp$^{116/117}$ proteins, but not with EqtII Trp^{45} or EqtII Trp^{149} (Figure 7). Kinetically, the change of tryptophan fluorescence of the wild-type and EqtII Trp$^{116/117}$ proteins is fast, completed within approx. 5 s. This correlates well with the observed binding of EqtII and mutants to SUV (Table 1), which was completed after 2 min. The time course of the increase was practically the same with Eqt II and EqtII Trp$^{116/117}$, and both rate constants increased with the lipid concentration (inset in Figure 7), since the number of sites available for toxin binding was larger. The intrinsic fluorescence of Eqt II and EqtII Trp$^{116/117}$ was also blue-shifted from 339 nm to 334 nm, whereas that of EqtII Trp^{45} and EqtII Trp^{149} was not (Figures 8A–8D). These effects were dependent on the lipid concentration (Figure 8E). The sum of the fluorescence intensities of the mutants in the presence of vesicles was $47.6\,\%$ of that of the wild-type, with a λ_{max} at 341 nm (Figure 8A). To ascertain whether the indolyl moieties of Eqt II and EqtII Trp$^{116/117}$ are indeed penetrating into the membrane, the lipid-confined quencher β-py-C_{10}-HPC was incorporated into the SUV. As expected, a strong lipid-dependent quenching was observed only with these two proteins (Figure 8 and Table 3), whereas the shift in λ_{max} was the same as that found with vesicles without quencher. The quenching efficiency was approx. 43 and $30\,\%$ for the wild-type and EqtII Trp$^{116/117}$ proteins respectively, indicating that in the wild-type, tryptophan residues other than those at position 116 and 117 were also quenched. Indeed, EqtII Trp^{45} and EqtII Trp^{149} could also have been quenched by pyrene, albeit to a much lower extent (Figure 8F and Table 3). This is not surprising, since pyrene, being a long-distance quencher of tryptophan (the Förster distance is 2.8 nm [35]), can also induce some quenching of tryptophan residues lying close to the membrane surface without actually being inserted into it.

DISCUSSION

Mutants EqtII Trp^{45}, EqtII Trp$^{116/117}$ and EqtII Trp^{149} might prove to be useful in the elucidation of the role of the peptide domains surrounding these tryptophan residues in the protein fold, and its interaction with the membrane. However, in the first

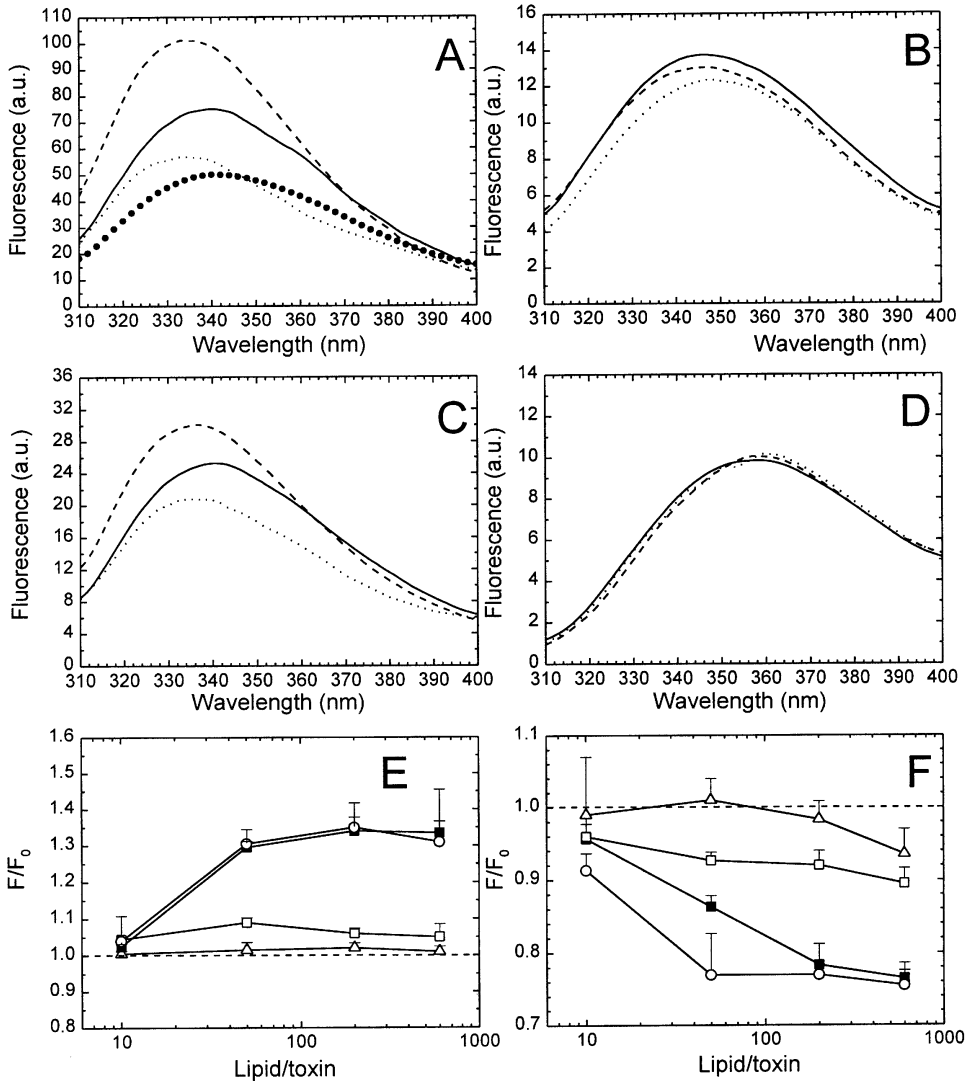

Figure 8 Effect of SUV on the tryptophan fluorescence of the wild-type and tryptophan mutants

Tryptophan fluorescence of 250 nM toxin (in 140 mM NaCl, 20 mM Tris/HCl, 1 mM EDTA, pH 8.5) was scanned in the absence (**A–D**, continuous lines) or the presence of SM/DPPC SUV (broken lines) or SM/DPPC/β-py-C_{10}-HPC SUV (dotted lines) at a lipid/toxin ratio of 600 at 25 °C. The excitation wavelength was set at 295 nm; slits were set at 5 nm. Proteins used were as follows: (**A**) the wild-type; (**B**) EqtII Trp^{45}; (**C**) EqtII $Trp^{116/117}$; and (**D**) EqtII Trp^{149}. The sum of tryptophan fluorescence of all mutants in the presence of SM/DPPC SUV is represented by the trace composed of large dots in (**A**). Dependence of the relative fluorescence intensity on the lipid/toxin molar ratio with SM/DPPC (1:1) SUV (**E**) or SM/DPPC/β-py-C_{10}-HPC (49:49:2) SUV (**F**) is shown, for the wild-type (■), EqtII Trp^{45} (□), EqtII $Trp^{116/117}$ (○) and EqtII Trp^{149} (△) proteins respectively. Data points represent the means + S.D. for three independent experiments.

instance an assessment of protein secondary structure was important, since substitutions of tryptophan with phenylalanine could cause conformational perturbations which, in the case of multiple substitutions, might have accumulated and substantially altered both the structure and activity of the mutants. The most commonly employed method for detecting structural changes introduced by site-directed mutagenesis is far-UV CD spectroscopy. Aromatic amino acids, especially tryptophan, contribute significantly to spectra not only in the near-UV, but also in the far-UV, regions [36,37]; therefore changing the number of tryptophan residues in the molecule usually affects its CD spectrum, even in the absence of real secondary structural changes. For these reasons, we decided to use IR spectroscopy instead, a method which is not sensitive to the number of tryptophan residues present [38]. By assessing the average composition with the use of FTIR spectroscopy, a large content of β-structure (β-sheet + turn) was revealed in all cases, comprising between 60 % and 70 % of the total secondary structure (Table 2), which seems to be a characteristic feature of all actinoporins [9,11,34]. The mutations introduced variable changes in the secondary structure, as well as some variation in the three-dimensional folding, indicated by changes in the ability to retain nitrogen-bound protons (Table 2).

Of the three mutants, EqtII $Trp^{116/117}$ was the least affected, having both the same average secondary structure and the same ability to retain protons as the wild-type. It was consistently found that, in most experiments, it behaved very similarly to EqtII. EqtII $Trp^{116/117}$ was only slightly less haemolytically active, and its lipid-binding ability was completely conserved. The emission wavelength maximum in the blue region and the low accessibility of tryptophan residues for acrylamide quenching or NBS modification suggested that these tryptophan residues are

placed in the hydrophobic interior of the protein, and are not exposed to the solvent. On the other hand, EqtII Trp^{149} was affected the most as a consequence of the mutation. Secondary structure analysis indicated that a substantial change had occurred, underlined by the fact that the β^2 band had a relative decrease of 22% while the random coil had a relative increase of 25%. This suggests that the mutant had undergone a degree of unfolding, which was confirmed by the fact that the ability to prevent exchange of nitrogen-bound protons was decreased to around one-sixth of that of the wild-type. As a result, the mutant was approximately 50 times less haemolytic than EqtII. The indolyl moiety of EqtII Trp^{149} was completely exposed to the solvent, as indicated by a red-shifted pattern of tryptophan fluorescence, and by acrylamide and NBS accessibility. EqtII Trp^{45} possessed some intermediate properties: as determined from FTIR spectroscopy measurements, its secondary structure was similar to that of the wild-type; however, its ability to prevent exchange of protons with deuterons was decreased by around 10%. Moreover, its functional properties and accessibility to acrylamide and NBS are intermediately placed between those of EqtII $Trp^{116/117}$ and EqtII Trp^{149}.

It is clear that the substitution of Trp^{45} or Trp^{149} with phenylalanine was more readily tolerated than alterations in the cluster of residues 112–117, which promoted a substantial change in the structural properties. Structural perturbations are often observed in proteins in which the mutated residues are located within the interior core. The possibility that tryptophan residues in the region 112–117 might form, or belong to, the hydrophobic core of EqtII must await the solution of the three-dimensional structure of the protein before confirmation is possible.

Single tryptophan mutants are useful in studies of protein–membrane interaction, since any blue shift and increase in tryptophan fluorescence can be interpreted as a transfer of tryptophan to a more hydrophobic environment, i.e. the lipid bilayer. Therefore with our set of mutants we could obtain information about the participation of three different parts of the EqtII molecule (Figure 1) to the binding to the lipids. All mutants bound with high affinity to lipid membranes, a common characteristic of actinoporins [4,39]. However, as determined by the fluorescence experiments, it seems probable that only Trp^{116} and Trp^{117} are transferred to the lipid bilayer. In fact, only EqtII $Trp^{116/117}$ showed an increase and blue shift of the fluorescence maximum, and was efficiently quenched by membrane-embedded quenchers, as found for the wild-type (Table 3). Because Trp^{112} is located in the immediate vicinity (Figure 1), it is likely that this also contributes similarly to the fluorescence increase, and hence it could account for the difference that is always present between the summed mutant spectra and the wild-type spectrum.

On the other hand, it seems likely that tryptophans at positions 45 and 149 do not interact with the membrane, since EqtII Trp^{45} and EqtII Trp^{149} exhibited no increase in intrinsic fluorescence and poor quenching with membrane-bound pyrene. The conclusion that they do not insert into the lipid bilayer, however, cannot be completely validated, especially in the case of EqtII Trp^{149}, because of the structural alterations observed. However, this would be consistent with a model proposed recently for membrane-bound toxin, derived from the study of 19 single cysteine mutants scattered along the sequence, in which the N-terminal helix, residues 105–120 and residues 144 and 160 are positioned within the lipid bilayer [8].

The proposed role for the cluster ^{112}Trp-Tyr-Ser-Asn-Trp-Trp^{117} of EqtII is reminiscent of that for perfringolysin O (PFO), a pore-forming toxin from *Clostridium perfringens* belonging to the large group of thiol-activated cytolysins. PFO forms large pores composed of approximately 30 monomers [40], and is organized into four domains [41]. One of the first steps of its pore-forming ability is the interaction of domain 4 with the lipid bilayer. The tip of this domain has a tryptophan cluster, ^{464}Trp-Glu-Trp-Trp^{467}, which enables binding to cholesterol, a specific acceptor for this group of proteins [42]. Upon a slight conformational change, which exposes hydrophobic side chains of neighbouring residues, the toxin may penetrate into the membrane. The cluster ^{112}Trp-Tyr-Ser-Asn-Trp-Trp^{117} of EqtII is in fact the only sequential resemblance that this molecule possesses to any other PFT. By analogy with PFO, it might interact with the membrane after slight conformational changes that enable its exposure. Whether the binding to the specific membrane acceptor, SM, promotes such a change remains to be demonstrated. Consistently with this notion, EqtII Trp^{45} and EqtII Trp^{149}, which are separate from the cluster, bind to membranes to a much lesser extent than the wild-type protein (Table 1).

In conclusion, binding of EqtII to the membranes is promoted by the tryptophan cluster (residues 112–117), which rapidly interacts with the membrane. This cluster is also important for maintaining the structure of EqtII. Tryptophan residues 116 and 117 can be used in further studies as donors of non-radiative energy for the excitation of fluorophores attached to cysteine, introduced by mutagenesis. Conformational changes occurring during the toxin binding could then be monitored by fluorescence resonance energy transfer from the tryptophan moiety to the extrinsic probe.

This work was supported by a grant from the Ministry of Science and Technology of the Republic of Slovenia and by grants of the Italian Consiglio Nazionale delle Ricerche (CNR) and Istituto Trentino di Cultura (ITC). G.A. was a recipient of an EMBO Short Term Fellowship.

REFERENCES

1 Gouaux, E. (1997) Curr. Opin. Struct. Biol. **7**, 566–573
2 Turk, T. (1991) J. Toxicol. Toxin. Rev. **10**, 223–262
3 Maček, P. (1992) FEMS Microbiol. Immunol. **105**, 121–130
4 Maček, P., Zecchini, M., Pederzolli, C., Dalla Serra, M. and Menestrina, G. (1995) Eur. J. Biochem. **234**, 329–335
5 Anderluh, G., Križaj, I., Štrukelj, B., Gubenšek, F., Maček, P. and Pungerčar, J. (1999) Toxicon **37**, 1391–1401
6 Zorec, R., Tester, M., Maček, P. and Mason, W. T. (1990) J. Membr. Biol. **118**, 243–249
7 Belmonte, G., Pederzolli, C., Maček, P. and Menestrina, G. (1993) J. Membr. Biol. **131**, 11–22
8 Anderluh, G., Barlič, A., Podlesek, Z., Maček, P., Pungerčar, J., Gubenšek, F., Zecchini, M., Serra, M. D. and Menestrina, G. (1999) Eur. J. Biochem. **263**, 128–136
9 Belmonte, G., Menestrina, G., Pederzolli, C., Križaj, I., Gubenšek, F., Turk, T. and Maček, P. (1994) Biochim. Biophys. Acta **1192**, 197–204
10 Anderluh, G., Pungerčar, J., Križaj, I., Štrukelj, B., Gubenšek, F. and Maček, P. (1997) Protein Eng. **10**, 751–755
11 Menestrina, G., Cabiaux, V. and Tejuca, M. (1999) Biochem. Biophys. Res. Commun. **254**, 174–180
12 Weiss, M. S., Abele, U., Weckesser, J., Welte, W., Schiltz, E. and Schulz, G. E. (1991) Science **254**, 1627–1630
13 Cowan, S. W., Schirmer, T., Rummel, G., Steiert, M., Ghosh, R., Pauptit, R. A., Jansonius, J. N. and Rosenbusch, J. P. (1992) Nature (London) **358**, 727–733
14 Doyle, D. A., Cabral, J. M., Pfuetzner, A. K., Gulbis, J. M., Cohen, S. L., Chait, B. T. and MacKinnon, R. (1998) Science **280**, 69–77
15 Forst, D., Welte, W., Wacker, T. and Diederichs, K. (1998) Nat. Struct. Biol. **5**, 37–46
16 Wallace, B. A. (1998) J. Struct. Biol. **121**, 123–141
17 Song, L., Hobaugh, M. R., Shustak, C., Cheley, S., Bayley, H. and Gouaux, J. E. (1996) Science **274**, 1859–1866
18 Gouaux, E. (1998) J. Struct. Biol. **121**, 110–122
19 Turk, T., Maček, P. and Gubenšek, F. (1992) Biochim. Biophys. Acta **1119**, 1–4
20 Pazos, I. F., Alvarez, C., Lanio, M. E., Martinez, D., Morera, V., Lissi, E. A. and Campos, A. M. (1998) Toxicon **36**, 1383–1393
21 Khoo, H. E., Fong, C. L., Yuen, R. and Chen, D. S. (1997) Biochem. Biophys. Res. Commun. **232**, 422–426

22 Anderluh, G., Pungerčar, J., Štrukelj, B., Maček, P. and Gubenšek, F. (1996) Biochem. Biophys. Res. Commun. **220**, 437–442
23 Michael, S. F. (1994) BioTechniques **16**, 410–412
24 Maček, P. and Lebez, D. (1988) Toxicon **26**, 441–451
25 Perkins, S. J. (1986) Eur. J. Biochem. **157**, 169–180
26 Lakowicz, J. R. (1983) Principles of Fluorescence Spectroscopy, Plenum Press, New York
27 Eftink, M. R. and Ghiron, C. A. (1981) Anal. Biochem. **114**, 199–227
28 Harrick, N. J. (1967) Internal Reflection Spectroscopy, Harrick Scientific Corporation, Ossining, New York
29 Menestrina, G. (2000) in Bacterial Toxins, Methods and Protocols (Holst, O., ed.), Humana Press, Totowa, NJ, in the press
30 Susi, H. and Byler, D. M. (1986) Methods Enzymol. **130**, 290–311
31 Tatulian, S. A., Hinterdorfer, P., Baber, G. and Tamm, L. K. (1995) EMBO J. **14**, 5514–5523
32 Tamm, L. K. and Tatulian, S. A. (1997) Q. Rev. Biophys. **30**, 365–429
33 Jackson, M. and Mantsch, H. H. (1995) Crit. Rev. Biochem. Mol. Biol. **30**, 95–120
34 Poklar, N., Lah, J., Salobir, M., Maček, P. and Vesnaver, G. (1997) Biochemistry **36**, 14345–14352
35 Wu, P. and Brand, L. (1994) Anal. Biochem. **218**, 1–13
36 Freskgard, P. O., Martensson, L. G., Jonasson, P., Jonsson, B. H. and Carlsson, U. (1994) Biochemistry **33**, 14281–14288
37 Woody, R. W. (1994) Eur. Biophys. J. **23**, 253–262
38 Goormaghtigh, E., Cabiaux, V. and Ruysschaert, J.-M. (1994) Subcell. Biochem. **23**, 363–403
39 Doyle, J. W. and Kem, W. R. (1989) Biochim. Biophys. Acta **987**, 181–186
40 Lesieur, C., Vecsey-Semjen, L., Abrami, L., Fivaz, M. and Van der Goot, F. G. (1997) Mol. Membr. Biol. **14**, 45–64
41 Rossjohn, J., Feil, S. C., McKinstry, W. J., Tweten, R. K. and Parker, M. W. (1997) Cell **89**, 685–692
42 Sekino-Suzuki, N., Nakamura, M., Mitsui, K. I. and Ohno-Iwashita, Y. (1996) Eur. J. Biochem. **241**, 941–947

Received 2 June 1999/30 September 1999; accepted 30 November 1999